

Application of X-ray Reflection Interface Microscopy in Thin-film Materials *

Zhan Zhang¹, Paul Zschack¹, Paul Fenter²

¹ X-ray Science Division, Argonne National Laboratory, Argonne, IL,
60439, USA

² Chemical Science & Engineering Division, Argonne National Laboratory,
Argonne, IL, 60439 USA

Nov 18, 2010, TWIG Meeting

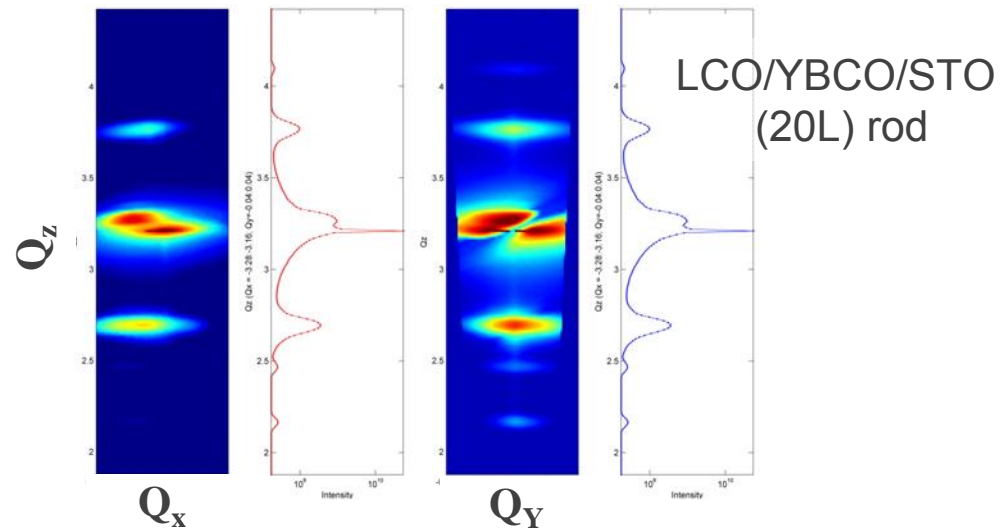
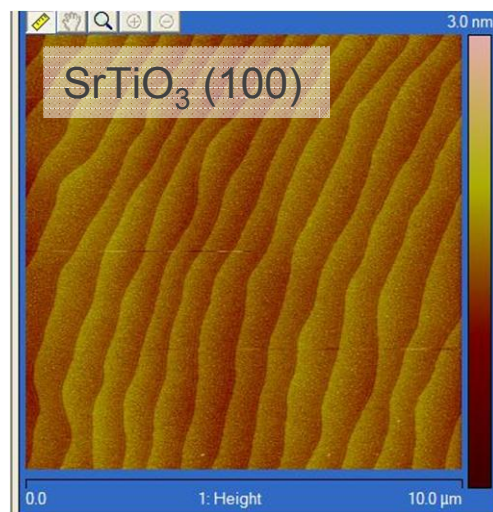
* This work is supported by Department of Energy, Office of Science, Office of Basic Energy Science, under Contract No. DE-AC02-06CH11357.

Outline

- Introduction
- X-ray reflection Interface Microscopy (XRIM)
 - Basics
 - Setups
- Examples
 - SrRuO₃/SrTiO₃
 - EuTiO₃/DyScO₃
 - Bi₂O₃ on STO
- Summary

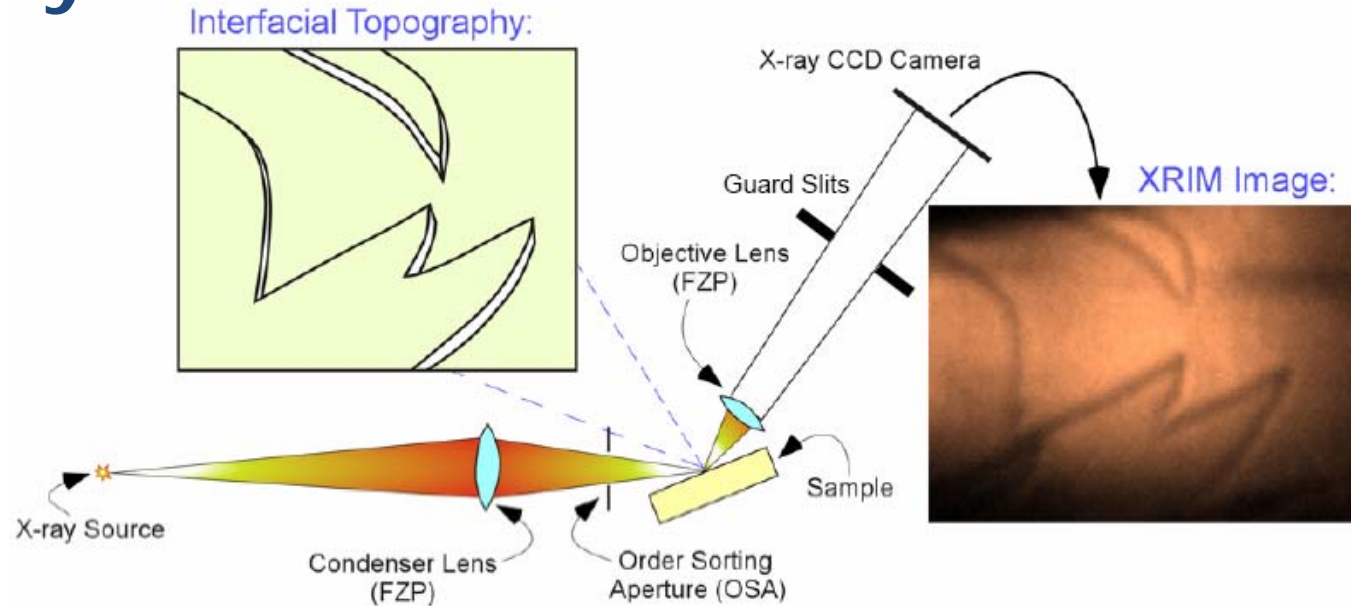
Introduction

- Imaging & scattering at surfaces and interfaces
 - Microscopy methods normally focus on topographical information
 - Scattering methods normally focus on structural information
 - Combination of the two methods could probe both at the same time

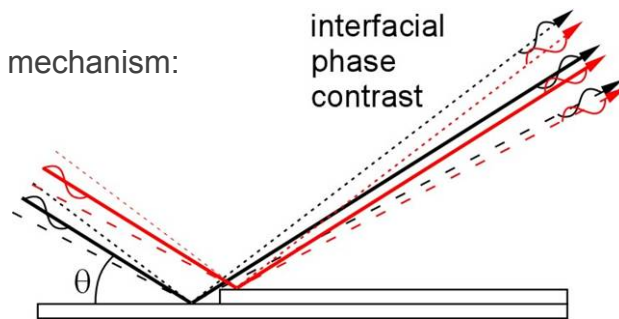


- Advantages of X-ray reflection surface/interface imaging
 - In-situ, real time measurements; probing buried interfaces, etc
 - Structure sensitive and potentially, element, valence state sensitive.
 - Quantitative analysis possible

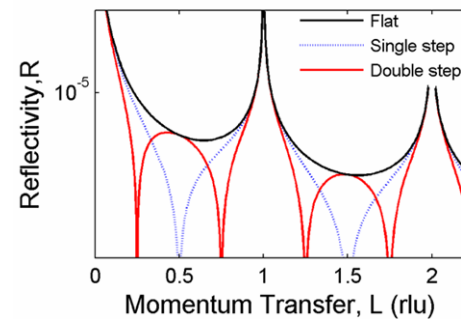
X-ray Reflection Interface Microscopy



Phase contrast mechanism:



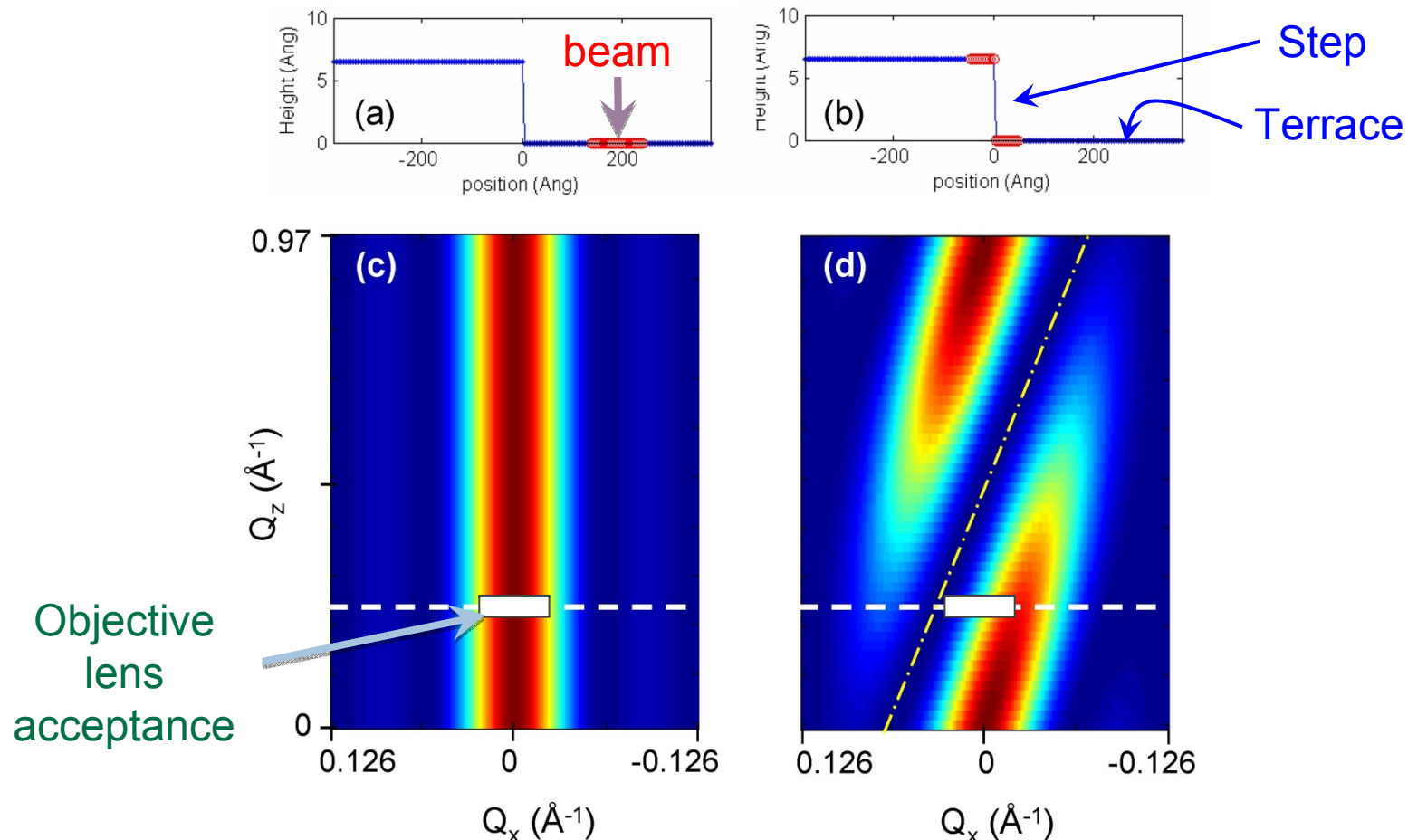
Intensity contrast at defects:



Characteristics:

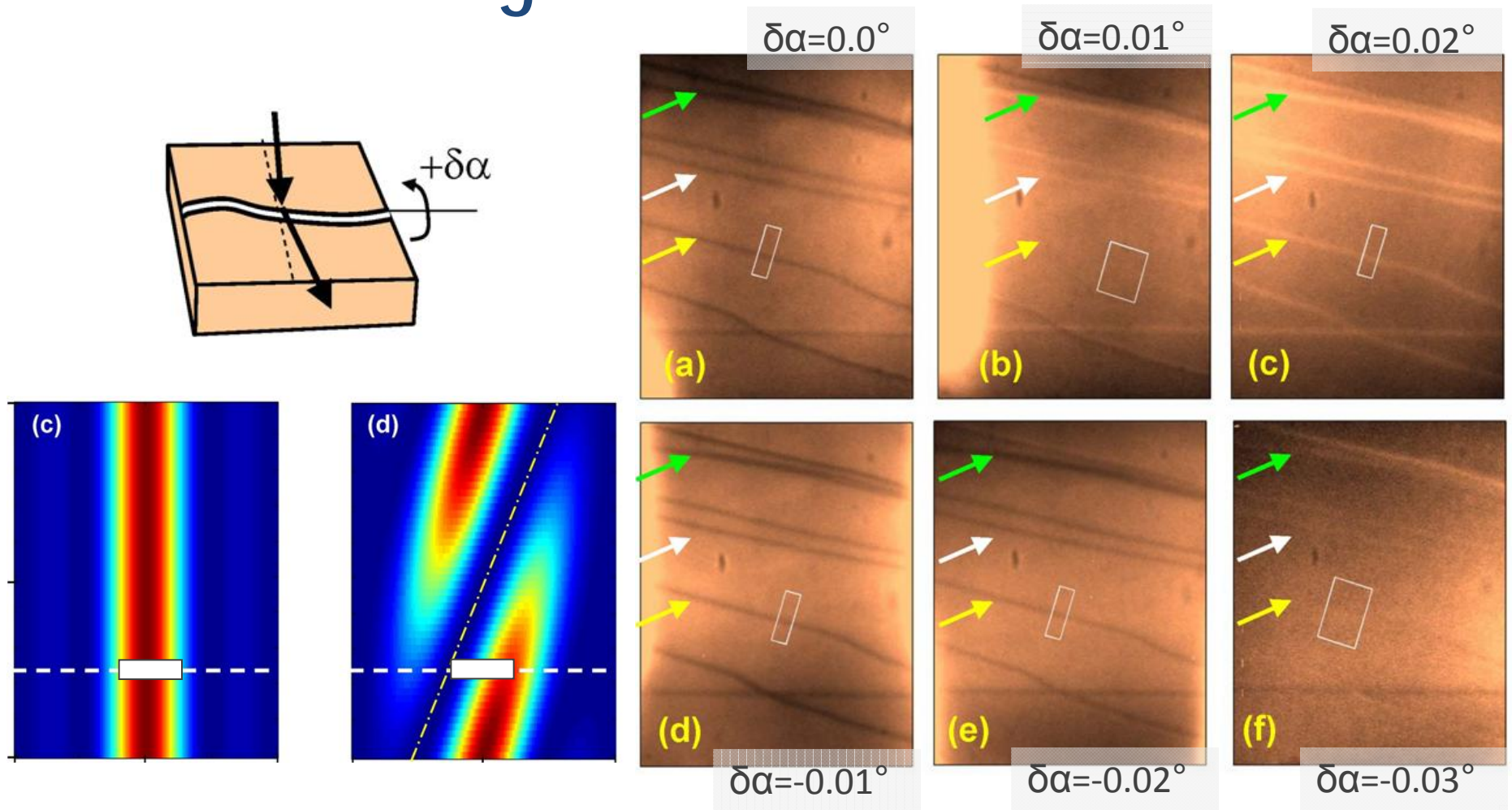
- Strong contrast ($\sim 100\%$), but weak reflected beam intensity ($R < 10^{-5}$)
- Sub-nm vertical sensitivity, but modest lateral resolution (~ 100 nm),

XRIM—Scattering View of Contrast Mechanism



- When the beam is on the terrace, the scattering intensity will all be accepted by the objective lens, i.e., the bright background;
- When the beam is over the step, some of the scattered intensity falls outside of the objective lens, i.e., the dark line appears.

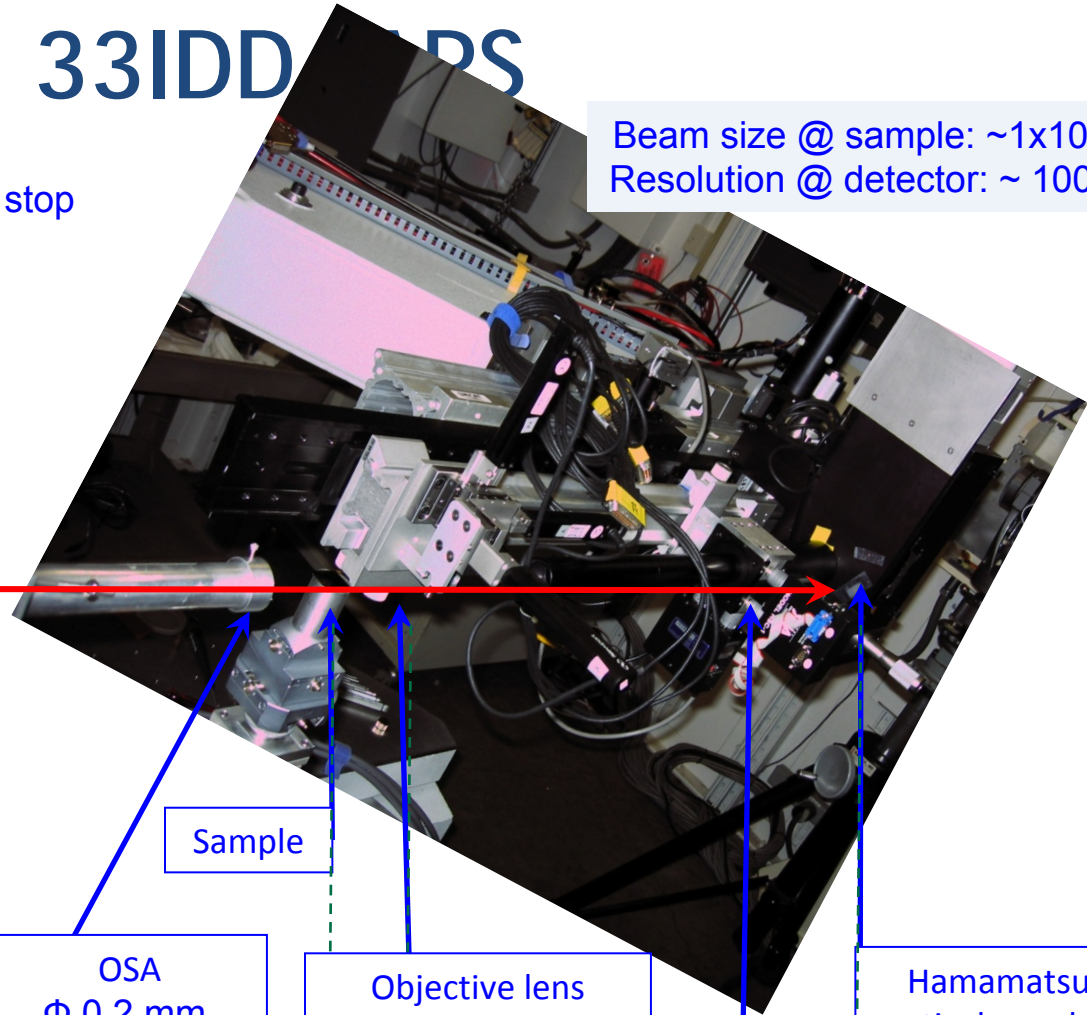
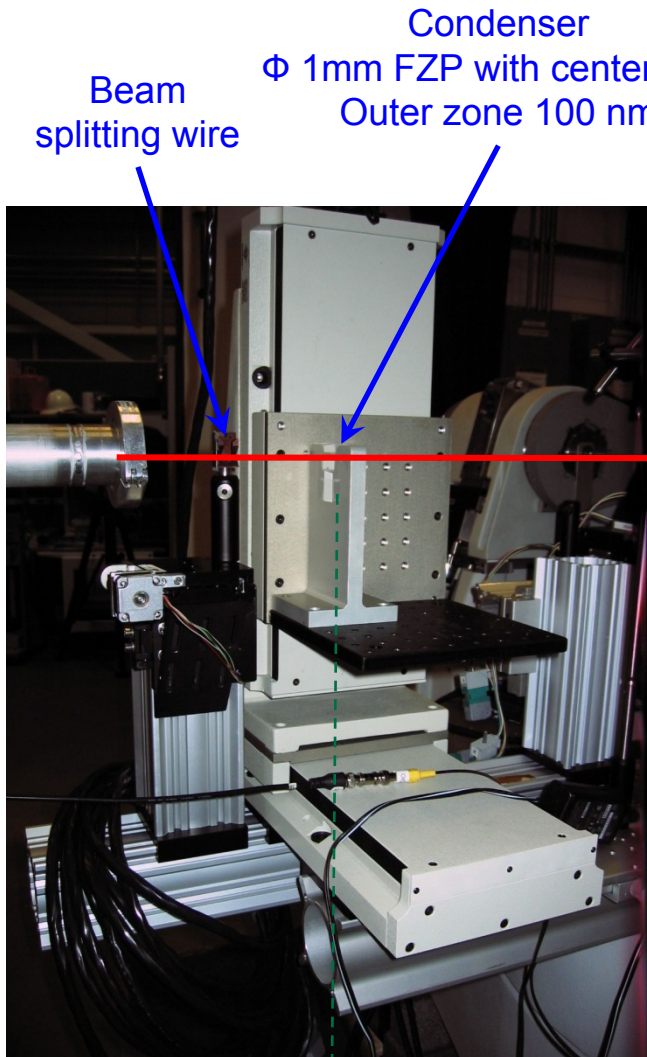
XRIM—Tuning the Contrast



The offset angle from the specular condition, $\delta\alpha$, controls the contrast between the terrace and the steps.

XRIM Setups at 33IDD

Beam size @ sample: $\sim 1 \times 10 \mu\text{m}$
 Resolution @ detector: $\sim 100 \text{ nm}$



Condenser
 $\Phi 1 \text{ mm}$ FZP with center stop
 Outer zone 100 nm

Beam splitting wire

Sample

OSA
 $\Phi 0.2 \text{ mm}$,
 $t=0.1 \text{ mm}$ PtIr

Objective lens
 $\Phi 80 \mu\text{m}$ FZP
 Outer zone 50 nm

OSA
 XIA slits

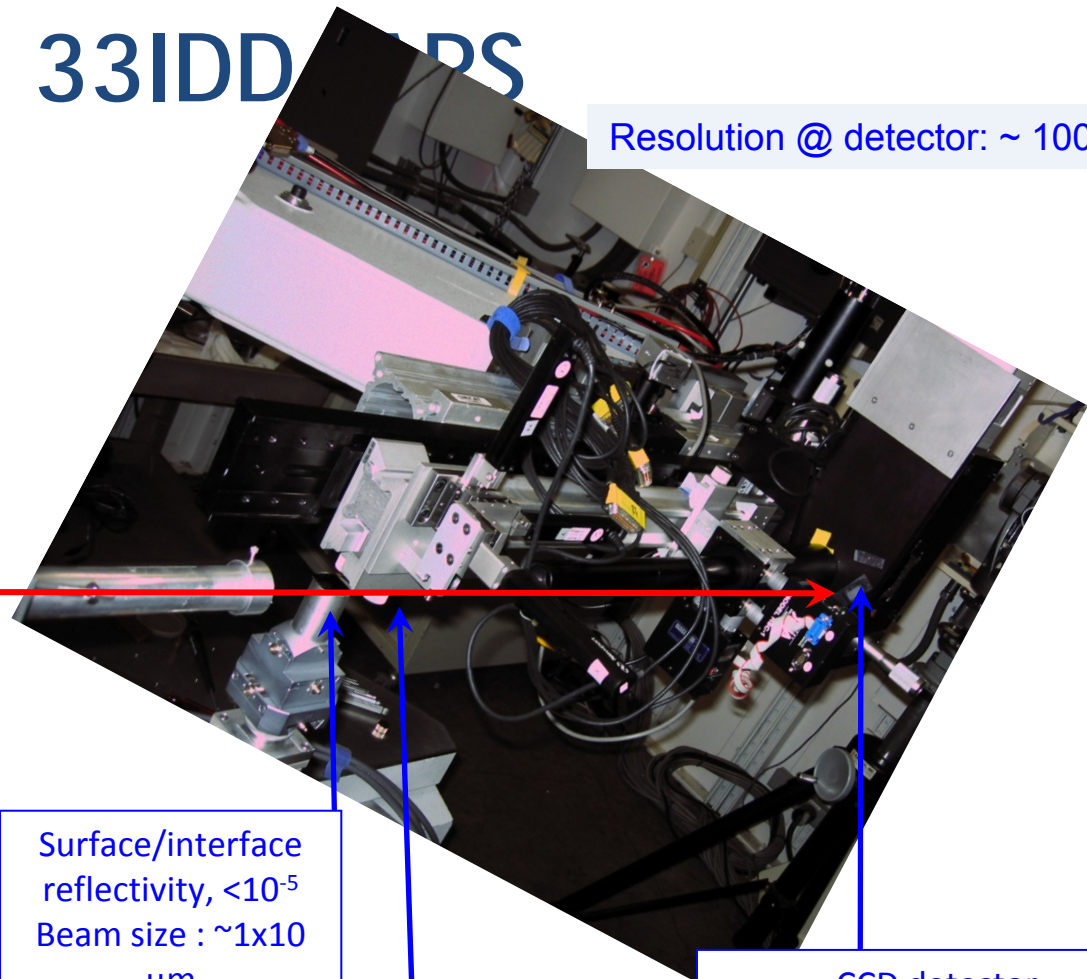
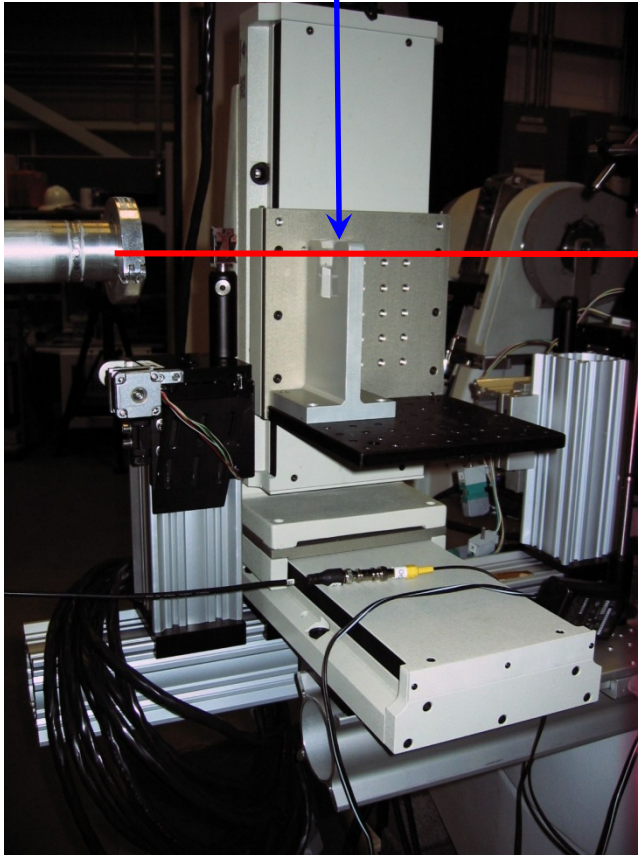
Hamamatsu
 optical coupled
 CCD detector

$\sim 60 \text{ m}$ to source $\sim 800 \text{ mm}$ $\sim 35 \text{ mm}$ $\sim 700 \text{ mm}$



XRIM Setups at 33IDD

Condenser FZP
Theoretical efficiency ~30%
Actual efficiency ~ 10%



Resolution @ detector: ~ 100 nm

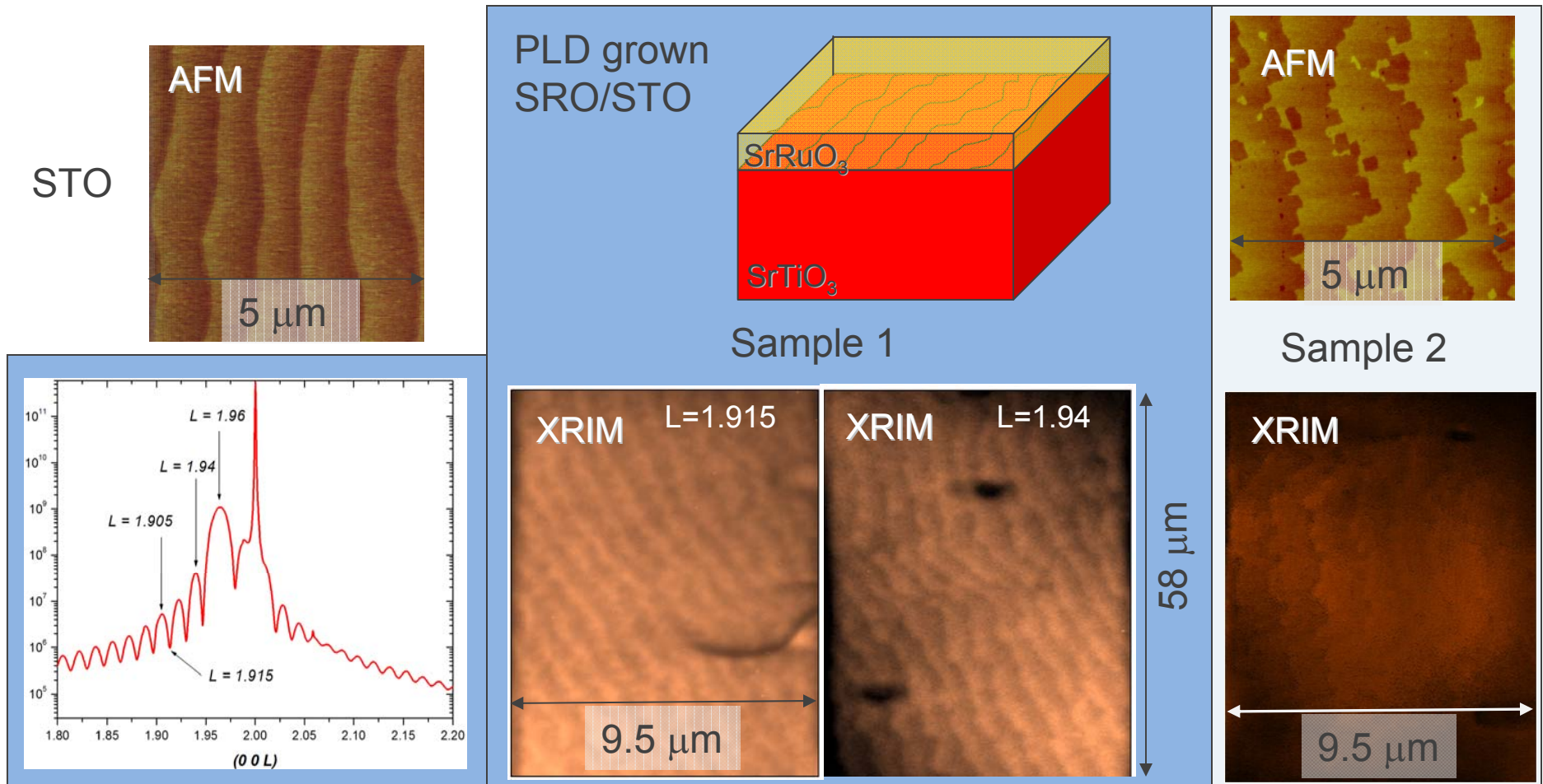
Surface/interface reflectivity, $<10^{-5}$
Beam size : $\sim 1 \times 10 \mu\text{m}$

Objective lens
Theoretical efficiency ~ 20%
Actual efficiency ~ 8%

CCD detector
1 X-ray photon ~ 1 count
Count time: 20s – 2000s
Actual resolution : 170 nm

Source size $\sim 16 \times 280 \mu\text{m}$, working energy 10keV, flux $\sim 10^{12}$ photon/s

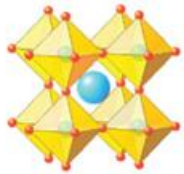
XRIM Measurements I - SRO/STO



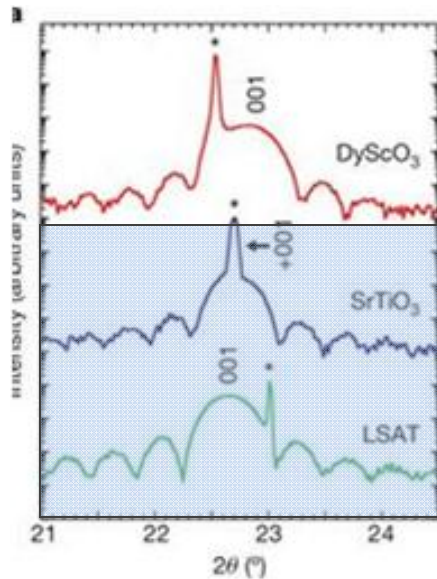
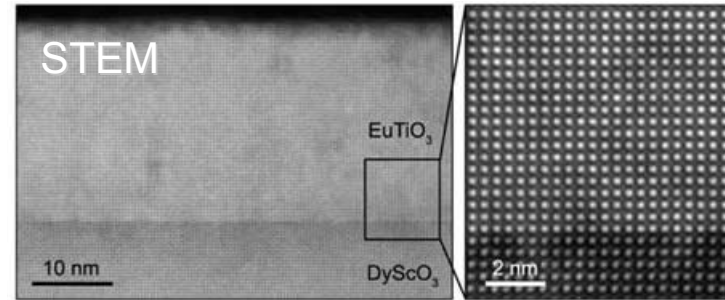
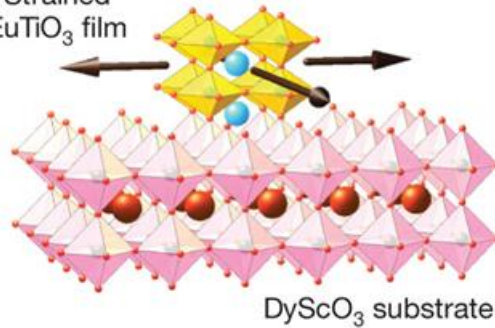
The steps on the STO surface (under $\sim 400 \text{ \AA}$ SRO film) can be seen on the sample 1, where the surface SRO features are smaller than the XRIM resolution. The zigzag steps on the SRO surface can be seen on sample 2 with XRIM as with AFM.

XRIM Measurements II - ETO/DSO

Bulk unstrained EuTiO_3



c Strained EuTiO_3 film



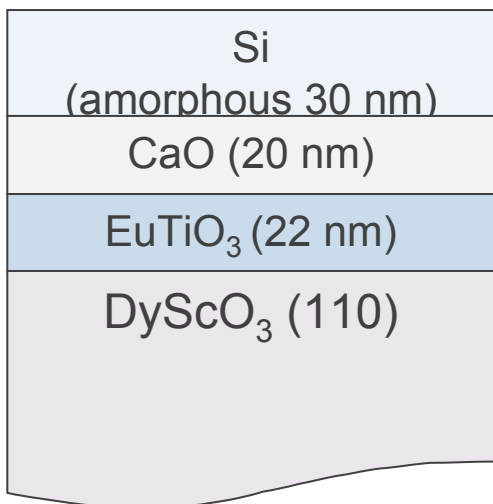
Surface normal direction:

$$\text{DSO (110): } c_{\text{DSC_bulk}} = 3.943 \text{ \AA}$$

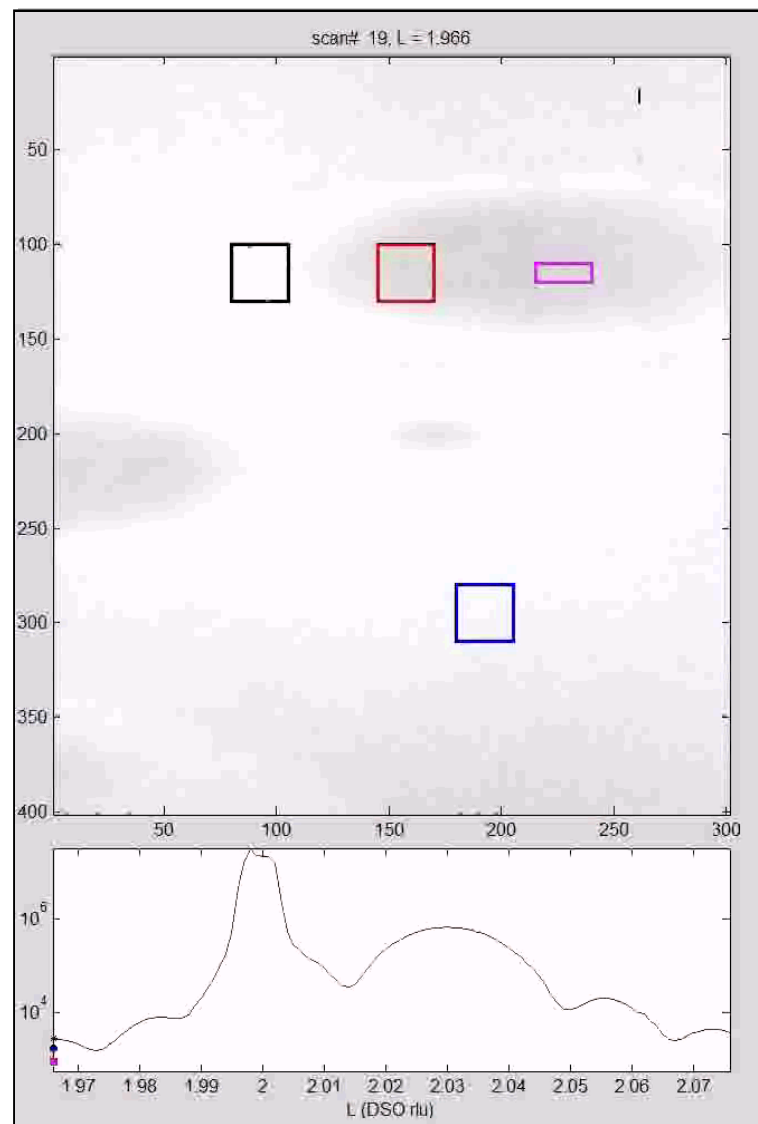
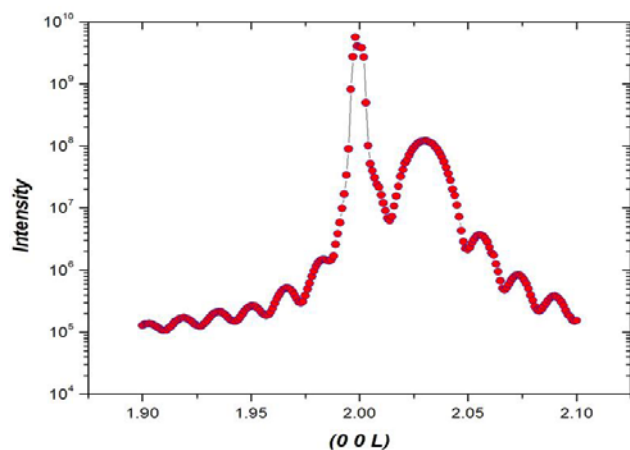
$$\text{ETO (100): } c_{\text{ETO_bulk}} = 3.905 \text{ \AA} \text{ vs. } c_{\text{ETO_film}} = 3.876 \text{ \AA}$$

In plane, ETO film is under $\sim 1.1\%$ biaxial tension to commensurate to the DSO substrate. Such ETO film is potentially both ferroelectric and ferromagnetic.

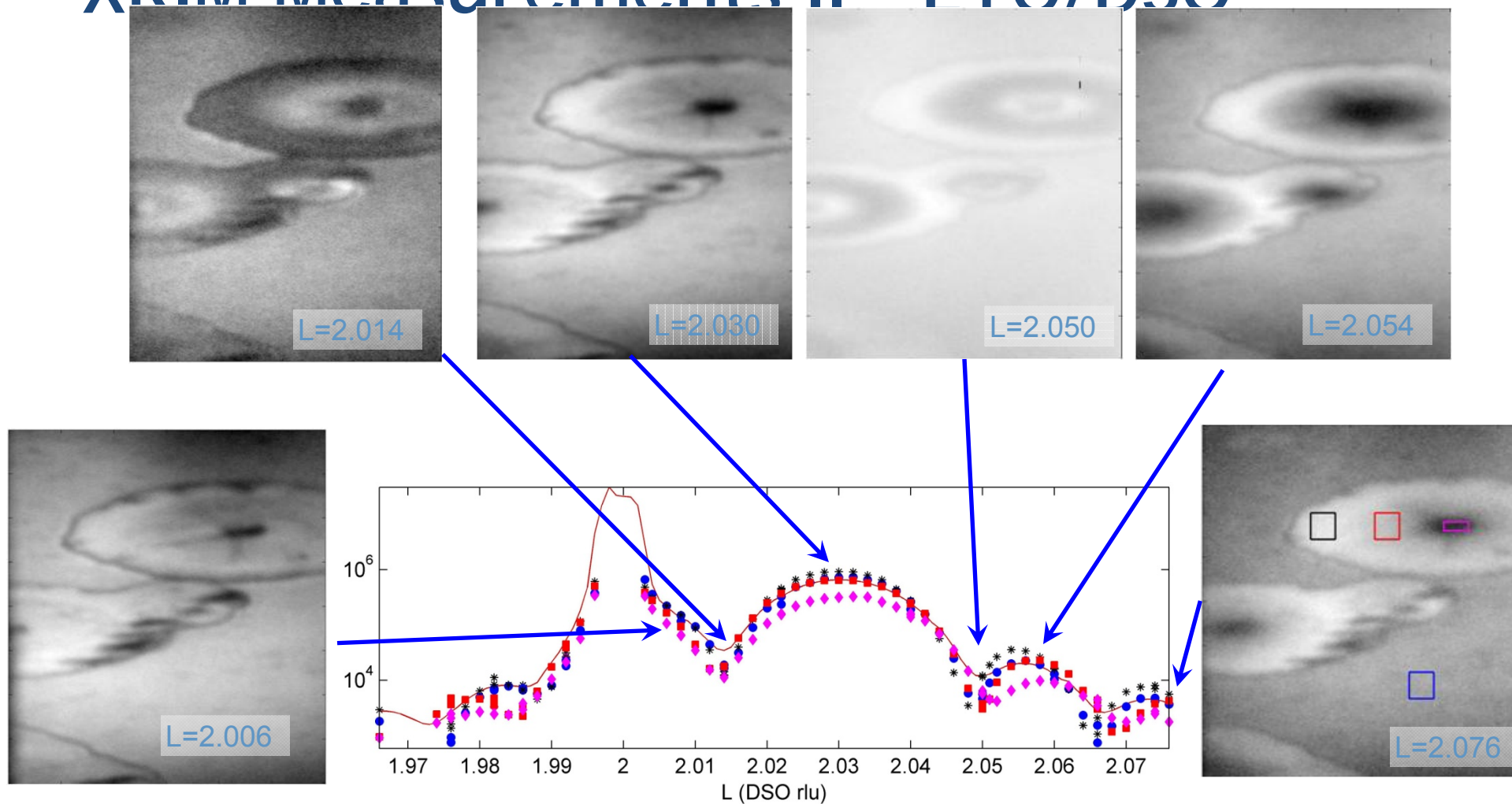
XRIM Measurements II - ETO/DSO



DSO: $c_{\text{DSO_bulk}} = 3.943 \text{ \AA}$
 ETO: $c_{\text{ETO_film}} = 3.884 \text{ \AA}$

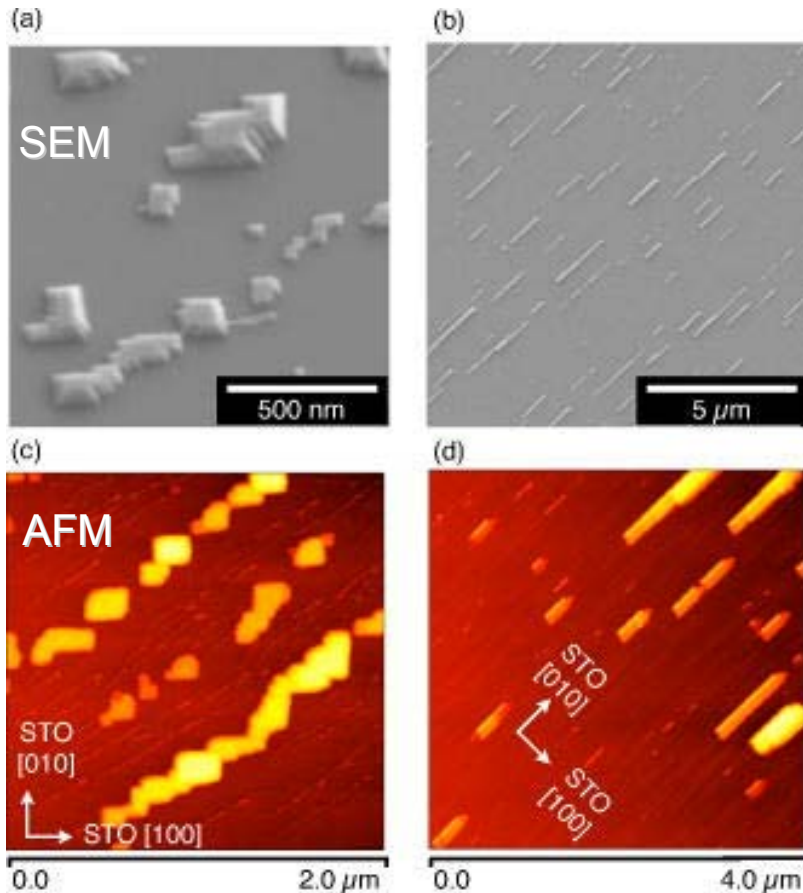


XRIM Measurements II - FTO/DSO



The center of the circular structure is thinner. Maybe some growth problem.

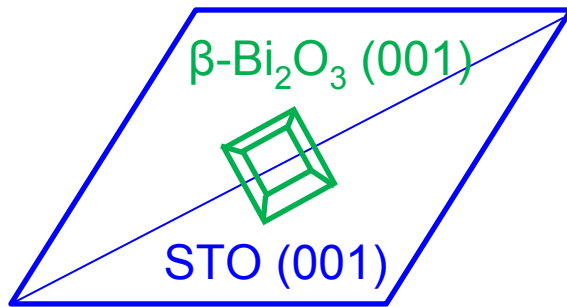
XRIM Measurements III - $\text{Bi}_2\text{O}_3/\text{STO}$



$\delta\text{-Bi}_2\text{O}_3$ is an important oxide ionic conductor, yet bulk phase is only stable in a narrow temperature range. By epitaxial growth on the slightly lattice mismatched oxide substrate, the $\delta\text{-Bi}_2\text{O}_3$ nano-structure or thin film can be stable in room temperature.

Images of $\delta\text{-Bi}_2\text{O}_3$ nanostructures on (001) SrTiO_3 . (a) and (c), SrTiO_3 miscut $<0.2^\circ$, nanoislands form with $\{101\}$ side-wall facets and coalesce along the substrate step edges. (b) and (d), On SrTiO_3 with 1° miscut along the $[100]$, nanowires form along the step edges. The heights of the nano-structures are around 100 nm.

XRIM Measurements III - Bi₂O₃/STO



Epitaxial Bi₂O₃ nano dots on STO (001) surface, a mixture of β and δ phases, with ~ 500 nm edge size.

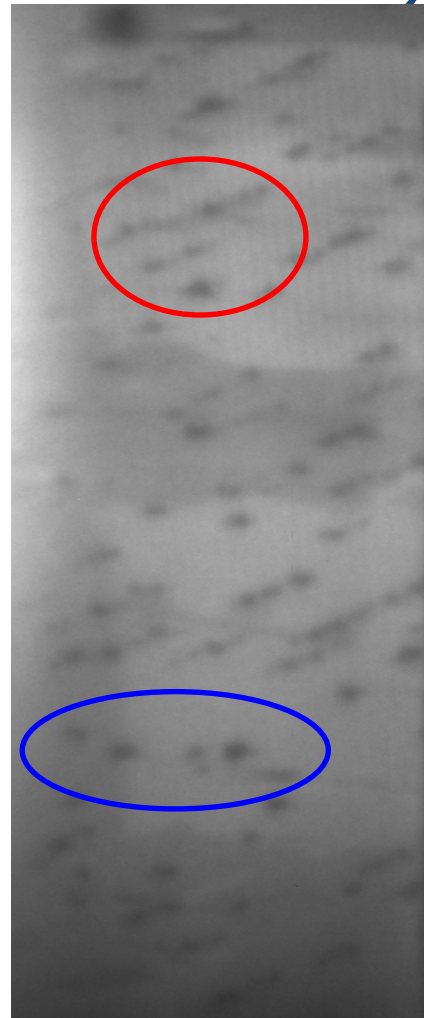
Surface normal direction:

β -Bi₂O₃: $c_0 = 5.62 \text{ \AA}$

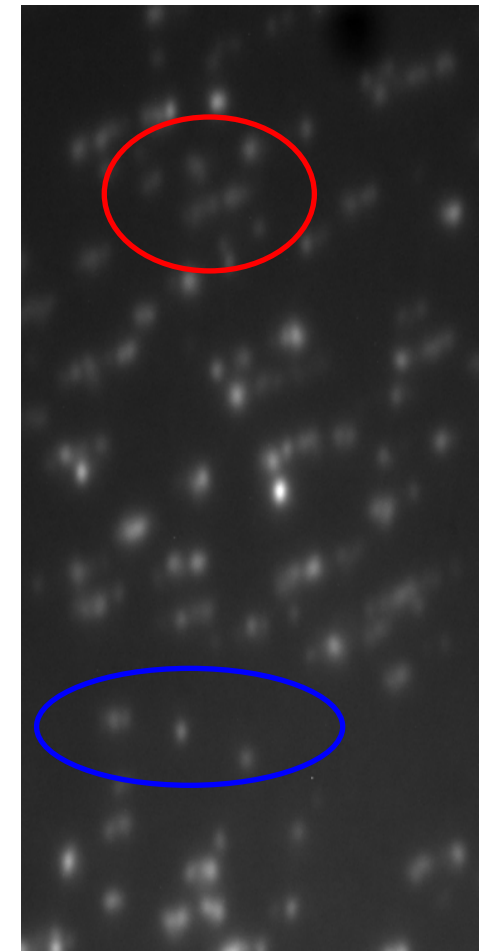
δ -Bi₂O₃: $c_0 = 5.531 \text{ \AA}$

STO: $c_0 = 3.905 \text{ \AA}$

- Near STO (002) Bragg peak, the nano dots appear to be dark.
- Near the β -Bi₂O₃ (002) Bragg peak, some of the dots light up.



L = 1.992 (STO)

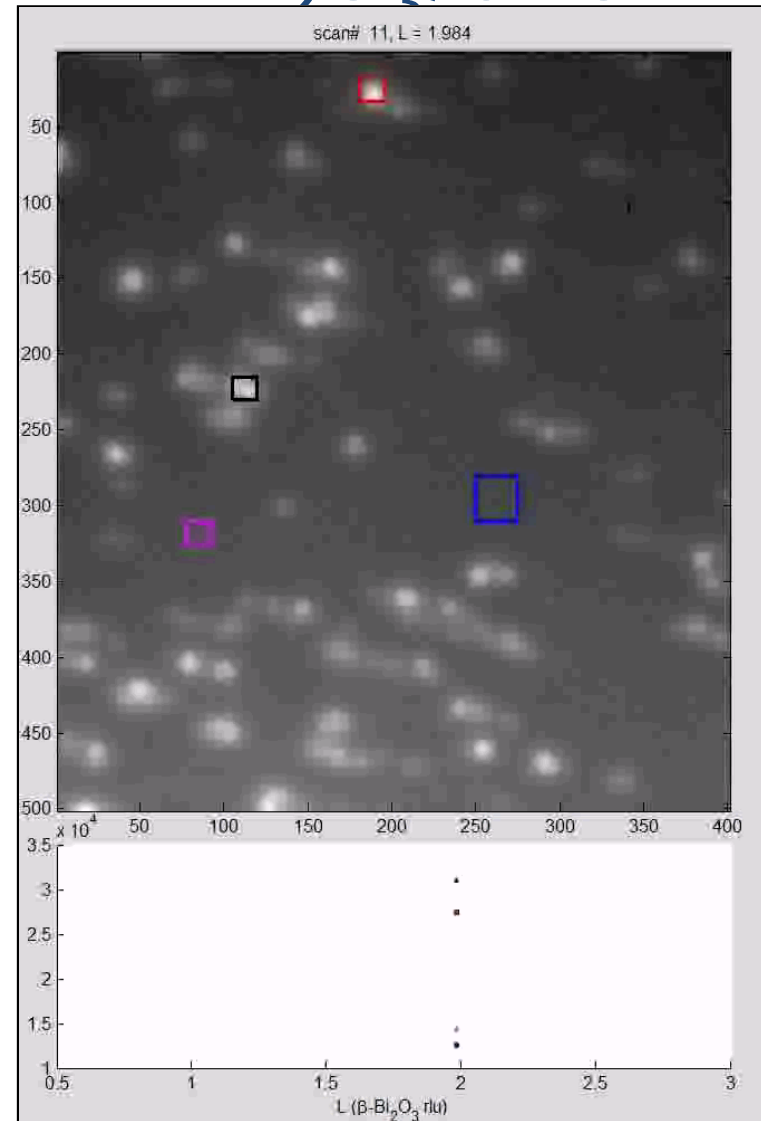


L = 2.002 (β -Bi₂O₃)

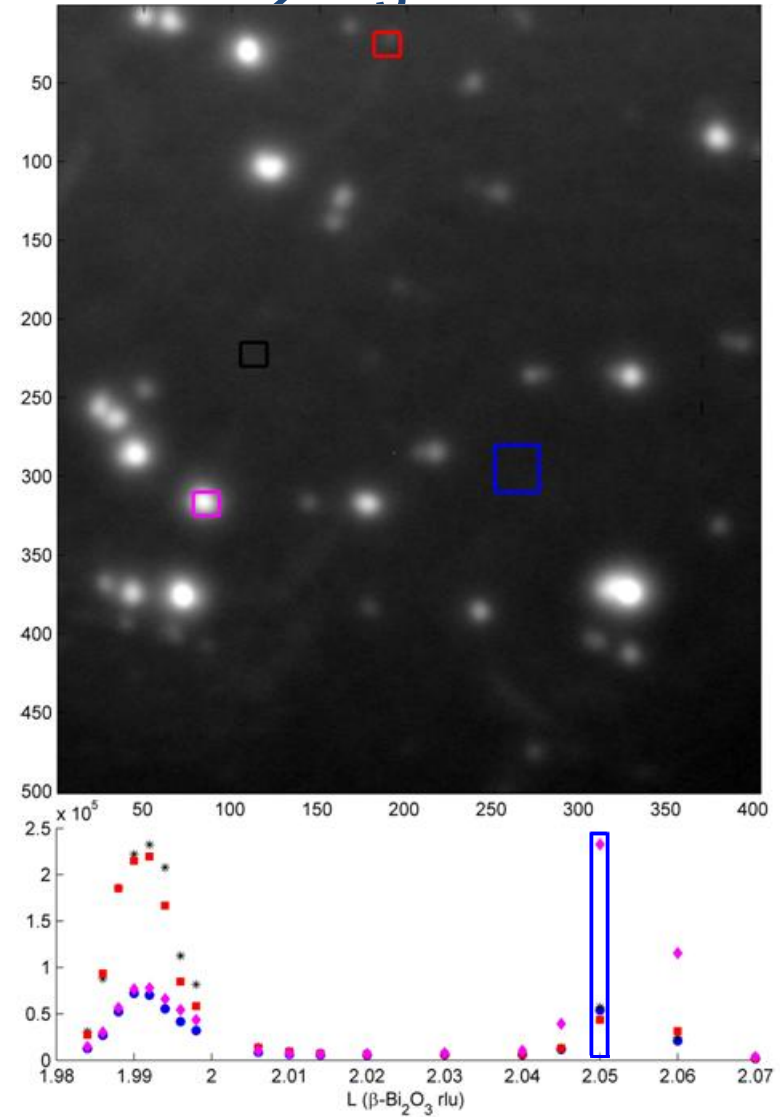
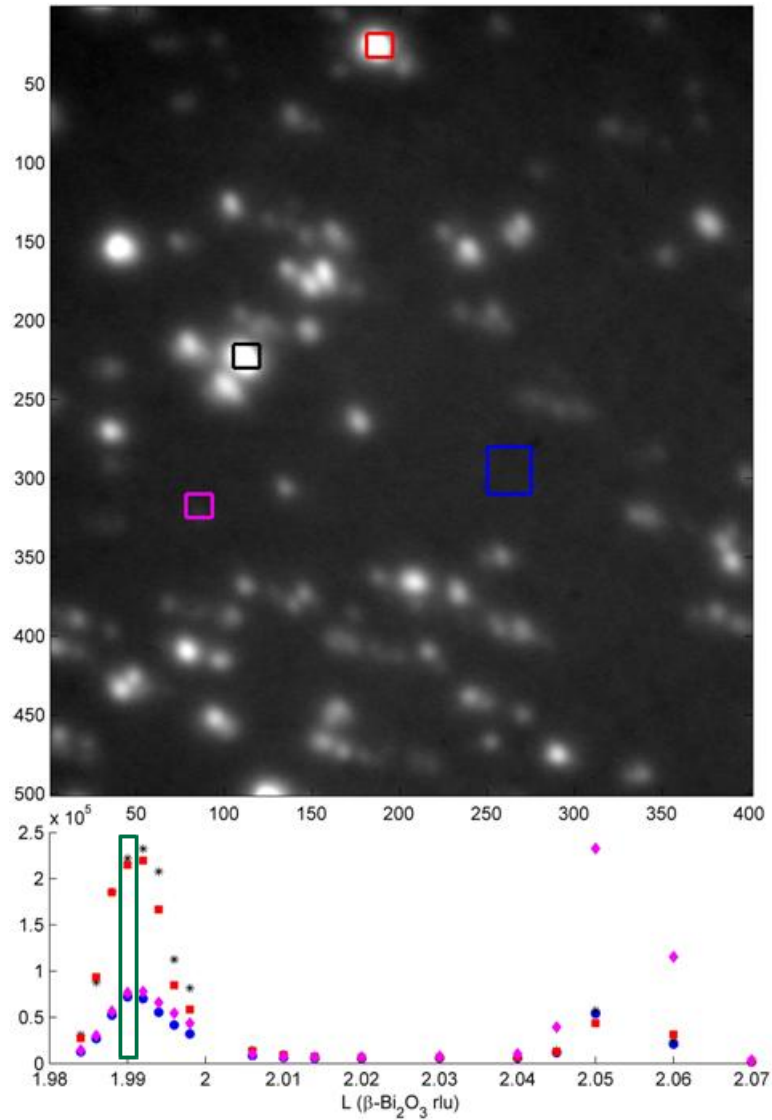
XRIM Measurements III - Bi₂O₃/STO

A series of XRIM images are taken along the surface normal direction, swiping through the β -Bi₂O₃ (002) Bragg peak and the δ -Bi₂O₃ (002) Bragg peak. The dots lighting up at the different reciprocal space positions are primarily different phases.

Bottom panel shows the integrated intensities of the boxes marked on the image.



XRIM Measurements III - Bi₂O₃/STO



Summary

- X-ray reflection interface microscopy is capable of imaging the surface, buried interface and thin film topography.
- The information carried in the XRIM images is quite rich. More effort is needed to decode them.
- With improved optics and detector, the in-situ, real time observations of many surface/interface processes, such as the thin film growth, surface dissolution and precipitation, could be realized.
- Combined with the X-ray scattering measurements, both the averaged and the localized information of the surface/interface could be quantitatively revealed.

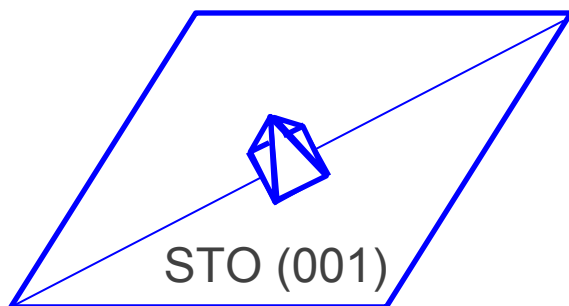
XRIM Further Developments

- In situ measurements (during growth, solid-liquid interface, etc)
- Improve the efficiency of the optics (from $<1\%$ \rightarrow 10-15%)
- Improve the resolution (<50 nm lateral resolution)
- Make it drop-in ready, easier to be combined with scattering measurements in the beamline.

Acknowledgement

- The XRIM data were measured at beamline 33ID at the Advanced Photon Source (APS) at Argonne National Laboratory (ANL). Use of the APS was supported by the U.S. Department of Energy, Office of Science, Office of Basic Energy Sciences (contract no. DE-AC02-06CH11357).
- The SRO/STO sample is from Gyula Eres, Christopher Rouleau, and Jonathan Tischler (Oak Ridge National Laboratory).
- The ETO/DSO sample is from June Hyuk Lee, Darrell G. Schlom (Cornell University), and John W. Freeland (APS, ANL).
- The Bi₂O₃/STO sample is from Danielle Proffit (Northwestern University & ANL) and Guo-Ren Bai (MSD, ANL), et al.
- The original development of XRIM was carried out at beamline 12ID, APS, ANL, with the help from Changyong Park, Vaibhav Kohli, and Jeff Catalano (CSE, ANL).

XRIM Measurements II - Bi₂O₃/STO



Nano-pyramid Bi₂O₃
epitaxial on STO (001)
surface.

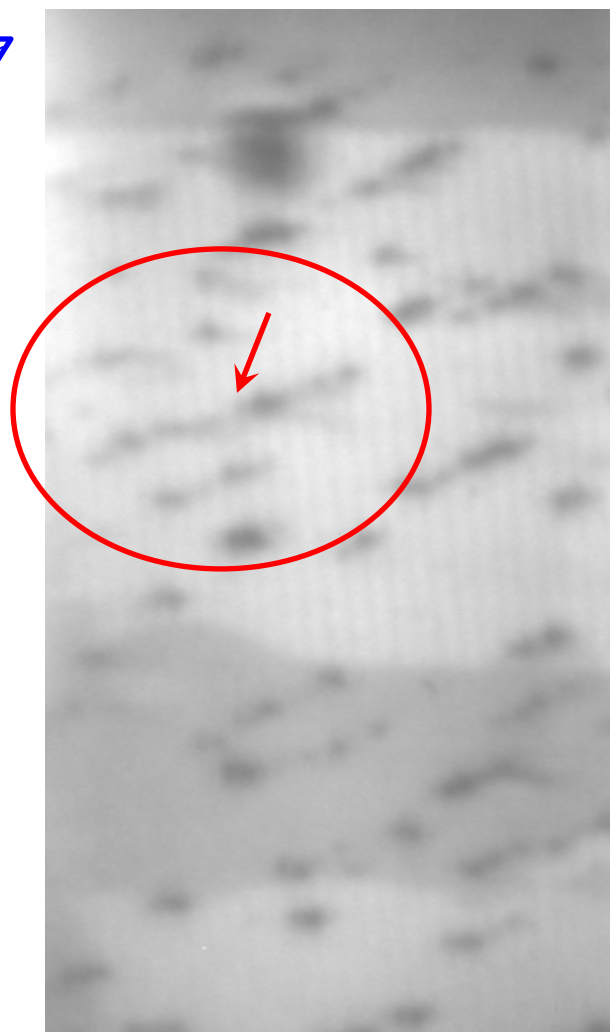
~ 500 nm edge size.

Surface normal direction:

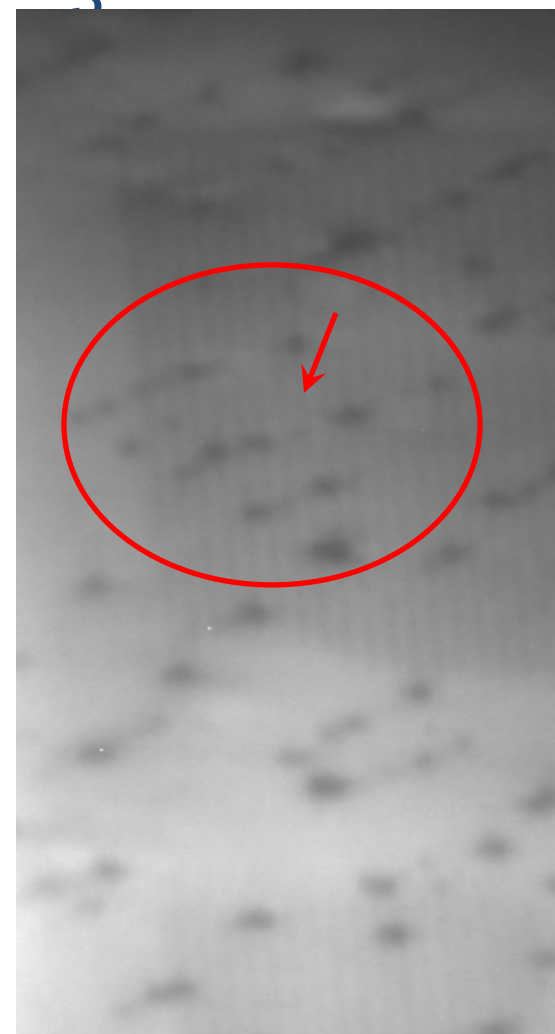
β -Bi₂O₃: $c_0 = 5.62 \text{ \AA}$

δ -Bi₂O₃: $c_0 = 5.531 \text{ \AA}$

STO: $c_0 = 3.905 \text{ \AA}$



$L = 1.99 \text{ (STO)}$



$L = 2.01 \text{ (STO)}$